A Study of T–S Model-Based SMC Scheme With Application to Robot Control

Yew-Wen Liang, *Member, IEEE*, Sheng-Dong Xu, *Student Member, IEEE*, Der-Cherng Liaw, *Senior Member, IEEE*, and Cheng-Chang Chen

***Abstract*—In light of the remarkable benefits and numerous applications of the Takagi–Sugeno (T–S) fuzzy system modeling method and the sliding mode control (SMC) technique, this paper aims to study the design of robust controllers for a set of second-order systems using a combination of these two approaches. The combined scheme is shown to have the merits of both approaches. It alleviates not only the online computational burden by using the T–S fuzzy system model to approximate the original nonlinear one (since most of the system parameters of the T–S model can be computed offline) but also preserves the advantages of rapid response and robustness characteristic of the classic SMC schemes. Moreover, the combined scheme does not need to online compute any nonlinear term of the original dynamics, and the increase in the number of fuzzy rules does not create extra online computational burdens for the scheme. The proposed analytical results are also applied to the control of a two-link robot manipulator and compared with the results using classic SMC design. Simulation results demonstrate the benefits of the proposed scheme.**

***Index Terms*—Robot manipulators, robust control, sliding-mode control (SMC), Takagi–Sugeno (T–S) fuzzy system model.**

I. Introduction

DUE to the efficiency and merits of solving complex nonlinear system identification and various control problems, fuzzy set theory and fuzzy system modeling have recently attracted considerable attention in both academic research and practical applications [3], [26], [27]. Among the existing fuzzy system modeling approaches, the so-called T–S fuzzy system model proposed by Takagi–Sugeno [26] has turned out to be one of the most popular modeling themes in the favor of its conceptual simplicity. The basic idea of the T–S approach is first to decompose a nonlinear system into several linear models according to different cases in which the associated linear models best fit the nonlinear one and, then, to aggregate each individual linear model into a single nonlinear one in terms of each model's membership functions. Although the concept is simple, the T–S fuzzy system model has been theoretically justified as a universal approximator [26], [27], which makes the T–S fuzzy system model become particularly useful, particularly when the nonlinear model is complicated [5], [9]–[11], [13], [14], [24]–[28], [30], [32]. Although a nonlinear control system can be well approximated by a suitably selected T–S fuzzy model, it creates additional model uncertainties between them. Therefore, a robust control scheme should be considered to efficiently compensate for such effects.

To compensate for the uncertainties and/or disturbances, several control system designs and analyses have been proposed. For instance, a class of control strategies is presented in terms of linear matrix inequality and parallel distributed compensation (PDC) technique [10], [27], [28]. Another robust control scheme, which is the use of the sliding mode control (SMC) technique, was recently proposed [11], [13], [19], [30], [32] in light of its remarkable advantages, including rapid response and robustness to model uncertainties and external disturbances [12], [16]. Due to these advantages, the SMC scheme has been widely employed to control a variety of systems [1], [2], [4], [6]–[8], [11]–[13], [15], [16], [18]–[21], [23], [24], [29], [30], [32]. For instance, Lin applied the terminal SMC approach to robot manipulators [20]. Yu *et al.* employed the PDC technique to derive a class of T–S fuzzy model-based SMC stabilizers [30]. In addition to the use of the PDC approach and the T–S fuzzy model-based SMC scheme, Hwang [11] also proposed an updating law to reduce the effect of uncertainties on system performance. In [32], Zheng *et al.* successfully used a combination of the T–S fuzzy modeling method and the SMC technique to study both the stabilization and the output tracking problems for a class of uncertain nonlinear systems, which need not be in triangular and parametric strict-feedback form. Lin *et al.* [19] further employed a similar approach to investigate the stabilization of uncertain fuzzy time-delay systems. It is noted that those two papers ([19] and [32]) impose an assumption that the control matrices B_i in each T–S fuzzy local model are identical. In [13], Khoo *et al.* adopted the PDC approach and the fuzzy extreme subsystem concept to deal with the reference trajectory tracking problem. In this paper, we will present a T–S fuzzy model-based SMC scheme that does not assume the control matrices B_i of each T–S local linear model to be identical. After the construction of the T–S fuzzy model, the upper bounds of the difference between the original and T–S models over each subregion will be offline computed. As a result, the proposed combined scheme not only greatly alleviates the online computational burden but it also preserves the same advantages of rapid response and robustness as those by using the classic SMC schemes. Moreover, it will be shown that the increase in the number of fuzzy rules does not create extra online computational burden to the scheme.

Manuscript received January 15, 2008; revised August 15, 2008. First published September 23, 2008; current version published October 31, 2008. This work was supported by the National Science Council, Taiwan, under Grants NSC 94-2623-7-009-005, NSC 95-2623-7-009-007-D, NSC 96-2623-7-009-013-D, and NSC 96-2221-E-009-228.

The authors are with the Department of Electrical and Control Engineering, National Chiao Tung University, Hsinchu 30010, Taiwan (e-mail: ywliang@cn.nctu.edu.tw).

Color versions of one or more of the figures in this paper are available online at http://ieeexplore.ieee.org.

Digital Object Identifier 10.1109/TIE.2008.2005138

The organization of this paper is as follows. Problem formulation and the main goal of this paper are given in Section II. It is followed by the description of the T–S fuzzy system model and the design of T–S fuzzy model-based SMC controllers. In Section IV, the obtained analytical results are applied to a two-link robot arm to demonstrate the benefits of the design. Finally, Section V gives the conclusion.

II. Problem Statement

Consider a set of nonlinear differential equations as given by

$$\dot{\mathbf{x}}_1 = \mathbf{x}_2 \tag{1}$$

$$\dot{\mathbf{x}}_2 = \mathbf{f}(\mathbf{x}) + G(\mathbf{x})(\mathbf{u} + \mathbf{d}). \tag{2}$$

Here, $\mathbf{x}_1 \in \mathbb{R}^n$, $\mathbf{x}_2 \in \mathbb{R}^n$, and $\mathbf{x} := (\mathbf{x}_1^T, \mathbf{x}_2^T)^T \in \mathbb{R}^{2n}$ denote the system state, $\mathbf{u} \in \mathbb{R}^n$ is the control input, $\mathbf{d} \in \mathbb{R}^n$ denotes the possible model uncertainties and external disturbances, $\mathbf{f}(\mathbf{x}) \in \mathbb{R}^n$ and $G(\mathbf{x}) \in \mathbb{R}^{n\times n}$ are the smooth functions, and $(\cdot)^{\mathrm{T}}$ denotes the transpose of a vector or a matrix.

The main goal of this paper is to synthesize a control law such that the system state will approach the desired trajectory even in the presence of external disturbances and/or model uncertainties, i.e., to design $\mathbf{u}$ such that $\mathbf{x}_1(t) \to \mathbf{x}_d(t)$ as $t \to \infty$, where $\mathbf{x}_d(t)$ is the desired trajectory.

III. Controller Design

Although considerable research has explored the problem described earlier (e.g., [9], [12], [16], [21], and [27]), in this paper, we will combine the T–S fuzzy approach and the SMC technique due to their remarkable advantages. First, it is known that a nonlinear model can be well approximated by a suitably selected T–S fuzzy system model, and most of the T–S fuzzy system model parameters can be off-line computed [26], [27]. Therefore, the T–S approach can alleviate much of the online computational burden and promote the opportunities for controller implementation, particularly for a complicated nonlinear system. Next, the SMC schemes are known to have the advantages of rapid response and robustness. Thus, the uncertainties resulting from the differences between the T–S fuzzy system and original nonlinear models might be easily compensated by a suitable SMC control law. Due to these remarkable benefits of the two aforementioned approaches, in the following, we will organize a class of T–S fuzzy model-based SMC controllers.

A. T–S Fuzzy System Model Description

It is known that a T–S fuzzy system model is generally described by a set of fuzzy implications according to the specific structure of the nonlinear systems (1) and (2). Suppose that there are p rules with the corresponding linear models, as described by

$$\dot{\mathbf{x}}_1 = \mathbf{x}_2 \tag{3}$$

$$\dot{\mathbf{x}}_2 = A_i\mathbf{x} + B_i\mathbf{u}, \qquad i = 1, \ldots, p. \tag{4}$$

Then, the T–S fuzzy system model can be constructed in the following forms to approximate the original nonlinear system:

$$\dot{\mathbf{x}}_1 = \mathbf{x}_2 \tag{5}$$

$$\dot{\mathbf{x}}_2 = \sum_{i=1}^{p} \alpha_i(\mathbf{x})(A_i\mathbf{x} + B_i\mathbf{u}) \tag{6}$$

where $\alpha_i(\mathbf{x}) \geq 0$ for all i, and $\sum_{i=1}^{p} \alpha_i(\mathbf{x}) = 1$. Following the T–S fuzzy system model representation as in (5) and (6), we can rewrite systems (1) and (2) as

$$\dot{\mathbf{x}}_1 = \mathbf{x}_2 \tag{7}$$

$$\dot{\mathbf{x}}_2 = \sum_{i=1}^{p} \alpha_i(\mathbf{x})A_i\mathbf{x} + \Delta\mathbf{f} + \left(\sum_{i=1}^{p} \alpha_i(\mathbf{x})B_i + \overline{\Delta G}\right)(\mathbf{u}+\mathbf{d}) \tag{8}$$

where $\Delta\mathbf{f} = \Delta\mathbf{f}(\mathbf{x}) := \mathbf{f}(\mathbf{x}) - \sum_{i=1}^{p} \alpha_i(\mathbf{x})A_i\mathbf{x}$, and $\overline{\Delta G} = \overline{\Delta G}(\mathbf{x}) := G(\mathbf{x}) - \sum_{i=1}^{p} \alpha_i(\mathbf{x})B_i$. To facilitate the design, we may further rewrite systems (7) and (8) in the following forms:

$$\dot{\mathbf{x}}_1 = \mathbf{x}_2 \tag{9}$$

$$\dot{\mathbf{x}}_2 = \sum_{i=1}^{p} \alpha_i(\mathbf{x})A_i\mathbf{x} + \Delta\mathbf{f} + \left(\sum_{i=1}^{p} \alpha_i(\mathbf{x})B_i\right) \cdot (I + \Delta G)(\mathbf{u} + \mathbf{d}) \tag{10}$$

where $\Delta G = (\sum_{i=1}^{p} \alpha_i(\mathbf{x})B_i)^{-1} \cdot \overline{\Delta G}$. In addition, we impose the following assumption for the existence of $(\sum_{i=1}^{p} \alpha_i(\mathbf{x})B_i)^{-1}$.

Assumption 1: The matrices $\sum_{i=1}^{p} \alpha_i(\mathbf{x})B_i$ are nonsingular for all possible states $\mathbf{x}$.

It is noted that the control matrix $G(\mathbf{x})$ is, in general, not constant over its workspace. Thus, the local matrices B_i given in (3) and (4) are distinct. If these matrices B_i are selected to be identical, for example, $B_i = B$ for some B and for all i, as those of [19] and [32], then $G(\mathbf{x})\mathbf{u}$ is written as $B(I + \Delta G)\mathbf{u}$. However, in case the variation of the control matrix $G(\mathbf{x})$ is large enough (i.e., $\max_{\mathbf{x}} \|\Delta G\|$ is close to or greater than one), the control performance using single B is generally not satisfactory. Thus, to better approximate the original nonlinear model, in this paper, we allow the local matrices B_i to be distinct.

B. SMC Controller Design

The SMC design is known to consist of two main steps ([15], [16]). The first step is the selection of an appropriate sliding surface, which should have the property that the desired performance can be achieved while the system state remains on the sliding surface. The next step is to organize a control law that forces the system state to reach the sliding surface in a finite amount of time and to make the sliding surface an invariant manifold. For the first step, we let

$$\mathbf{e} = \mathbf{x}_1 - \mathbf{x}_d \tag{11}$$

and select the sliding surface as

$$\mathbf{s} = \dot{\mathbf{e}} + K\mathbf{e} = \mathbf{0} \tag{12}$$

where $K = \mathrm{diag}\{k_1, \ldots, k_n\} > 0$. It is obvious that the objective of the design (i.e., $\mathbf{e} \to \mathbf{0}$) can be achieved if the system state remains on the sliding surface.

For the second step, it is noted in (9)–(12) that

$$\begin{aligned}\dot{\mathbf{s}} &= \ddot{\mathbf{e}} + K\dot{\mathbf{e}} \\ &= \ddot{\mathbf{x}}_1 - \ddot{\mathbf{x}}_d + K\dot{\mathbf{e}} \\ &= -\ddot{\mathbf{x}}_d + K\dot{\mathbf{e}} + \sum_{i=1}^{p} \alpha_i(\mathbf{x}) A_i \mathbf{x} + \Delta\mathbf{f} \\ &\quad + \left(\sum_{i=1}^{p} \alpha_i(\mathbf{x}) B_i\right)(I + \Delta G)(\mathbf{u} + \mathbf{d}).\end{aligned} \tag{13}$$

According to the SMC design procedure (e.g., [15] and [16]), we choose

$$\mathbf{u} = \mathbf{u}^{\mathrm{eq}} + \mathbf{u}^{\mathrm{re}} \tag{14}$$

$$\mathbf{u}^{\mathrm{eq}} = \left(\sum_{i=1}^{p} \alpha_i(\mathbf{x}) B_i\right)^{-1} \cdot \left[-\sum_{i=1}^{p} \alpha_i(\mathbf{x}) A_i \mathbf{x} + \ddot{\mathbf{x}}_d - K\dot{\mathbf{e}}\right]. \tag{15}$$

It follows that

$$\begin{aligned}\dot{\mathbf{s}} = \Delta\mathbf{f} &+ \left(\sum_{i=1}^{p} \alpha_i(\mathbf{x}) B_i\right)(I + \Delta G)(\mathbf{u}^{\mathrm{re}} + \mathbf{d}) \\ &+ \left(\sum_{i=1}^{p} \alpha_i(\mathbf{x}) B_i\right) \Delta G \cdot \mathbf{u}^{\mathrm{eq}}.\end{aligned} \tag{16}$$

In order to force the system state to reach the sliding surface in a finite amount of time, we impose the following assumption, where $\|\cdot\|$ denotes the Euclidean norm.

Assumption 2: There exist nonnegative functions $\rho(\mathbf{x}, t)$ and $\sigma(\mathbf{x}, t)$ such that

$$\left\| \Delta\mathbf{f} + \left(\sum_{i=1}^{p} \alpha_i(\mathbf{x}) B_i\right)[(I + \Delta G) \cdot \mathbf{d} + \Delta G \cdot \mathbf{u}^{\mathrm{eq}}] \right\| \le \rho(\mathbf{x}, t) \tag{17}$$

$$\sqrt{n} \left\| \left(\sum_{i=1}^{p} \alpha_i(\mathbf{x}) B_i\right) \Delta G \left(\sum_{i=1}^{p} \alpha_i(\mathbf{x}) B_i\right)^{-1} \right\| \le \sigma(\mathbf{x}, t) < 1. \tag{18}$$

It is noted that, although the inequality given by (17) requires the information of $\mathbf{u}^{\mathrm{eq}}$, $\rho(\mathbf{x}, t)$ can be easily obtained after the calculation of $\mathbf{u}^{\mathrm{eq}}$ since the upper bound of $\|\Delta\mathbf{f}\|$ and $\|\Delta G\|$ can be estimated offline. Under Assumption 2, we choose

$$\mathbf{u}^{\mathrm{re}} = -\frac{\rho(\mathbf{x}, t) + \eta}{1 - \sigma(\mathbf{x}, t)} \left(\sum_{i=1}^{p} \alpha_i(\mathbf{x}) B_i\right)^{-1} \cdot \mathrm{sgn}(\mathbf{s}) \tag{19}$$

where η is a positive constant. Since $\|\mathrm{sgn}(\mathbf{s})\| \le \sqrt{n}$, it follows from (16), (19), and Assumption 2 that

$$\begin{aligned}\mathbf{s}^{\mathrm{T}}\dot{\mathbf{s}} &\overset{(17)}{\le} \rho(\mathbf{x}, t)\|\mathbf{s}\| + \mathbf{s}^{\mathrm{T}} \left(\sum_{i=1}^{p} \alpha_i(\mathbf{x}) B_i\right)(I + \Delta G)\mathbf{u}^{\mathrm{re}} \\ &\overset{(19)}{\le} \rho(\mathbf{x}, t)\|\mathbf{s}\| - \frac{\rho(\mathbf{x}, t) + \eta}{1 - \sigma(\mathbf{x}, t)} \cdot \mathbf{s}^{\mathrm{T}} \\ &\quad \cdot \left[I + \left(\sum_{i=1}^{p} \alpha_i(\mathbf{x}) B_i\right) \Delta G \left(\sum_{i=1}^{p} \alpha_i(\mathbf{x}) B_i\right)^{-1}\right] \\ &\quad \cdot \mathrm{sgn}(\mathbf{s}) \\ &\overset{(18)}{\le} \rho(\mathbf{x}, t)\|\mathbf{s}\| - \frac{\rho(\mathbf{x}, t) + \eta}{1 - \sigma(\mathbf{x}, t)} \left(\sum_{i=1}^{p} |s_i| - \sigma(\mathbf{x}, t)\|\mathbf{s}\|\right) \\ &\le \rho(\mathbf{x}, t)\|\mathbf{s}\| - \frac{\rho(\mathbf{x}, t) + \eta}{1 - \sigma(\mathbf{x}, t)} (\|\mathbf{s}\| - \sigma(\mathbf{x}, t)\|\mathbf{s}\|) \\ &\le \eta \cdot \|\mathbf{s}\|.\end{aligned} \tag{20}$$

That is, the system state will reach the sliding surface in a finite amount of time. From the discussions earlier, we hence have the following result.

Theorem 1: Suppose that Assumptions 1 and 2 hold. Then, the tracking performance for systems (1) and (2) with control laws (14), (15), and (19) can be achieved.

Note that the T–S fuzzy model-based controllers, as presented earlier, have an important characteristic. They do not need to online compute the nonlinear term $\mathbf{f}(\mathbf{x})$ and the inverse dynamics of $G(\mathbf{x})$, which is inevitable for the conventional SMC schemes (e.g., [16]), as given in the following:

$$\mathbf{u} = -G^{-1}(\mathbf{x}) \cdot [\mathbf{f}(\mathbf{x}) + K\dot{\mathbf{e}} - \ddot{\mathbf{x}}_d + (\lambda + \eta) \cdot \mathrm{sgn}(\mathbf{s})] \tag{21}$$

where $\eta > 0$, and λ is an upper bound of $\|G(\mathbf{x})\mathbf{d}\|$. Instead, for the T–S-type SMC controllers, the system parameters A_i and B_i, and the upper bounds for $\|\Delta\mathbf{f}\|$, $\|\Delta G\|$, and $\sigma(\mathbf{x}, t)$, as stated in Assumption 2, of the T–S-type SMC controllers can be off-line computed. Thus, the T–S-type approach may significantly alleviate online computational burden for controller computation and thus promote the opportunity for controller implementation, particularly when the system dynamics is complicated.

IV. Application to Robot Manipulators

Consider a two-link robot manipulator, as shown in Fig. 1. The governing equations for this system have the following form (e.g., [17], [20], [22], [28], and [31])

$$M(\mathbf{q})\ddot{\mathbf{q}} + C(\mathbf{q}, \dot{\mathbf{q}})\dot{\mathbf{q}} + \mathbf{g}(\mathbf{q}) = \boldsymbol{\tau} + \mathbf{d} \tag{22}$$

where $\mathbf{q} = (q_1, q_2)^{\mathrm{T}} \in \mathbb{R}^2$, $\boldsymbol{\tau} = (\tau_1, \tau_2)^T \in \mathbb{R}^2$ and $\mathbf{d} \in \mathbb{R}^2$ denote the generalized coordinates (radians), the control torques (N-m) and possible external disturbances, respectively. $M(\mathbf{q})$ is the moment of inertia, $C(\mathbf{q}, \dot{\mathbf{q}})$ contains the Coriolis and the centripetal forces, and $\mathbf{g}(\mathbf{q})$ is the gravitational force.

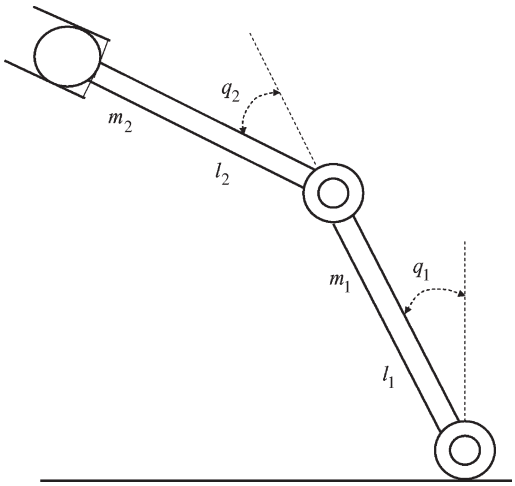

Fig. 1. Two-link robot manipulator.

Denote $(\cdot)_{ij}$ the (i,j)-entry of a matrix. These terms are expressed as stated in the following [28]:

$$(M(\mathbf{q}))_{11} = (m_1 + m_2)l_1^2 \tag{23}$$

$$(M(\mathbf{q}))_{12} = (M(\mathbf{q}))_{21} = m_2 l_1 l_2 (c_1 c_2 + s_1 s_2) \tag{24}$$

$$(M(\mathbf{q}))_{21} = m_2 l_1 l_2 (c_1 c_2 + s_1 s_2) \tag{25}$$

$$(M(\mathbf{q}))_{22} = m_2 l_2^2 \tag{26}$$

$$C(\mathbf{q}, \dot{\mathbf{q}}) = m_2 l_1 l_2 (c_1 s_2 - s_1 c_2) \begin{pmatrix} 0 & -\dot{q}_2 \\ -\dot{q}_1 & 0 \end{pmatrix} \tag{27}$$

$$\mathbf{g}(\mathbf{q}) = \begin{pmatrix} -(m_1 + m_2) l_1 g s_1 \\ -m_2 l_2 g s_2 \end{pmatrix} \tag{28}$$

where m_1 and m_2 (in kilograms) are link masses, l_1 and l_2 (in meters) are link lengths, $g = 9.8$ (m/s^2) is the acceleration due to gravity, and $c_i = \cos(q_i)$ and $s_i = \sin(q_i)$ for $i = 1, 2$. Let $\mathbf{x}_1 = (x_1, x_2)^{\mathrm{T}} = (q_1, q_2)^{\mathrm{T}}$, $\mathbf{x}_2 = (x_3, x_4)^{\mathrm{T}} = (\dot{q}_1, \dot{q}_2)^{\mathrm{T}}$, $\mathbf{u} = \boldsymbol{\tau}$ and $\mathbf{f}(\mathbf{x}) = (f_1(\mathbf{x}), f_2(\mathbf{x}))^{\mathrm{T}}$. It is not difficult to check that system (22) can be transformed into the form of (1) and (2) with

$$\begin{aligned} f_1(\mathbf{x}) &= m_2 l_1 l_2 a_1 a_3 x_3^2 - m_2 l_2^2 a_1 x_4^2 \\ &\quad + (m_1 + m_2) g s_1 / (l_1 a_2) - m_2 g a_3 s_2 / (l_1 a_2) \\ f_2(\mathbf{x}) &= m_2 l_1 l_2 a_1 a_3 x_4^2 + (m_1 + m_2) \\ &\quad \cdot \left(l_1^2 a_1 x_3^2 - g a_3 s_1 / (l_2 a_2) + g s_2 / (l_2 a_2) \right) \\ G(\mathbf{x}) &= \begin{pmatrix} 1/\left(l_1^2 a_2\right) & -a_3/(l_1 l_2 a_2) \\ -a_3/(l_1 l_2 a_2) & (m_1 + m_2)/\left(m_2 l_2^2 a_2\right) \end{pmatrix} \end{aligned}$$

where $a_1 = (s_1 c_2 - c_1 s_2)/a_2$, $a_2 = (m_1 + m_2 - m_2 a_3^2)$, and $a_3 = c_1 c_2 + s_1 s_2$. Since $|a_3| = |c_1 c_2 + s_1 s_2| = |\cos(x_1 - x_2)| \leq 1$, we have $a_2 > m_1 > 0$. By direct inspection, $\mathrm{trace}(G(\mathbf{x})) = (1/(l_1^2 a_2)) + ((m_1 + m_2)/(m_2 l_2^2 a_2)) > 0$ and $\det(G(\mathbf{x})) = ((m_1 + m_2 - m_2 a_3^2)/(m_2 l_1^2 l_2^2 a_2^2)) = (1/(m_2 l_1^2 l_2^2 a_2)) > 0$ since $a_2 > 0$. Those imply that $G(\mathbf{x})$ is always a positive definite matrix for all $\mathbf{x}$. It follows that all the matrices B_i, obtained from $G(\mathbf{x})$ at a specific operating point, are positive definite. Thus, $\sum_{i=1}^{p} \alpha_i(\mathbf{x}) B_i$ is always a positive definite matrix for any $\mathbf{x}$. Assumption 1 is hence satisfied.

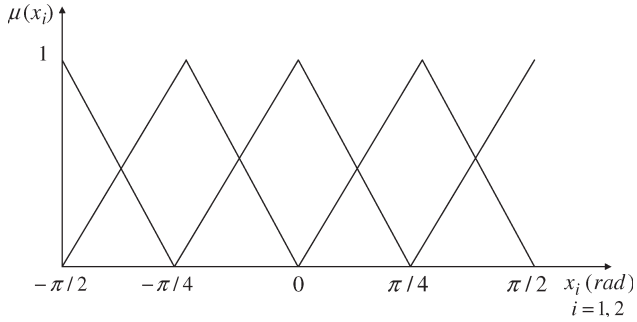

Fig. 2. Selected operating points and the membership functions for the case of $n_1 = n_2 = 5$.

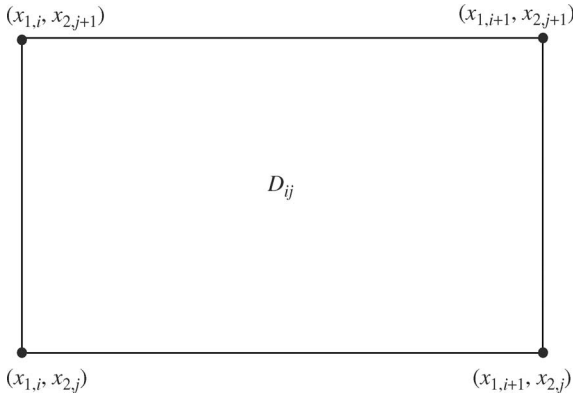

Fig. 3. Four adjacent operating points being triggered at each time instant.

To derive an appropriate T–S fuzzy system model to approximate the original nonlinear dynamics, a set of operating points will be selected for the construction of the associated linear models. These operating points are selected from the possible workspace, so that the motion of the robot can be well approximated by using a convex combination of the associated linear models. For demonstration, we assume that $m_1 = m_2 = 1$ and $l_1 = l_2 = 1$, and the angular positions x_1 and x_2 are constrained to be $-\pi/2 \leq x_i \leq \pi/2$, where $i = 1, 2$. The operating points are chosen in the form of $\{\mathbf{x}_{ij} = (x_{1,i}, x_{2,j}, 0, 0)^{\mathrm{T}} | i = 1, \ldots, n_1 \text{ and } j = 1 \cdots, n_2\}$, where $\{x_{1,1}, \ldots, x_{1,n_1}\}$ and $\{x_{2,1}, \ldots, x_{2,n_2}\}$ are two selected partitions of $[-\pi/2, \pi/2]$. In this example, we employ the triangular membership functions for both x_1 and x_2, where the case of $n_1 = n_2 = 5$ is shown in Fig. 2. Since the T–S-type controller uses only two premise variables x_1 and x_2, it therefore triggers at most four rules (i.e., at most four linear models) at each time instant, as shown in Fig. 3, where $D_{ij} = \{\mathbf{x} \mid x_{1,i} \leq x_1 \leq x_{1,i+1} \text{ and } x_{2,j} \leq x_2 \leq x_{2,j+1}\}$. Thus, it does not create an extra online computational burden if the partition for the regions of x_1 and x_2 is made finer. However, since the maximum value of a function over a smaller subregion is smaller than or equal to that of the same function over the whole region, it follows that a finer partition for the regions of x_1 and x_2 will result in a smaller magnitude of $\sigma(\mathbf{x}, t)$ and $\rho(\mathbf{x}, t)$, as stated in Assumption 2. Thus, the control magnitude will be smaller so that the physical control magnitude constraint is easier to fulfill for practical applications if the partition of x_1 and x_2 is made finer. To investigate the effects of the partition, in the following, we consider two cases of which one of the partitions is finer than the other.

TABLE I
ESTIMATED UPPER BOUNDS OF $\sigma(\mathbf{x},t)$ AND $\|\Delta\mathbf{f}\|_\infty$ IN THE REGION D_{ij}, WHERE $i,j=1,\ldots,4$

	D_{11},D_{44}	D_{12},D_{43}	D_{13},D_{42}	D_{14},D_{41}	D_{21},D_{34}	D_{22},D_{33}	D_{23},D_{32}	D_{24},D_{31}
$\sigma(\mathbf{x},t)$	0.4055	0.1302	0.1595	0.1244	0.1302	0.4055	0.125	0.1595
$\|\|\Delta\mathbf{f}\|\|_\infty$	2.5629	2.3826	2.3818	1.8818	2.3899	4.4399	4.4399	2.4891

TABLE II
ESTIMATED UPPER BOUNDS OF $\sigma(\mathbf{x},t)$ AND $\|\Delta\mathbf{f}\|_\infty$ IN THE REGION D_{ij}, WHERE $i,j=1,\ldots,8$

	D_{11},D_{88}	D_{12},D_{87}	D_{13},D_{86}	D_{14},D_{85}	D_{15},D_{84}	D_{16},D_{83}	D_{17},D_{82}	D_{18},D_{81}
$\sigma(\mathbf{x},t)$	0.1294	0.07	0.0499	0.0645	0.0538	0.0645	0.0499	0.07
$\|\|\Delta\mathbf{f}\|\|_\infty$	1.166	1.5069	1.7451	1.6475	1.3724	1.2165	1.2387	1.2706
	D_{21},D_{78}	D_{22},D_{77}	D_{23},D_{76}	D_{24},D_{75}	D_{25},D_{74}	D_{26},D_{73}	D_{27},D_{72}	D_{28},D_{71}
$\sigma(\mathbf{x},t)$	0.07	0.1294	0.07	0.0499	0.0645	0.0538	0.0645	0.0499
$\|\|\Delta\mathbf{f}\|\|_\infty$	1.5702	1.017	1.3987	1.6568	1.6285	1.357	1.202	1.2057
	D_{31},D_{68}	D_{32},D_{67}	D_{33},D_{66}	D_{34},D_{65}	D_{35},D_{64}	D_{36},D_{63}	D_{37},D_{62}	D_{38},D_{61}
$\sigma(\mathbf{x},t)$	0.0499	0.07	0.1294	0.07	0.0499	0.0645	0.0538	0.0645
$\|\|\Delta\mathbf{f}\|\|_\infty$	1.6729	1.391	0.976	1.3336	1.5997	1.6146	1.3674	1.1816
	D_{41},D_{58}	D_{42},D_{57}	D_{43},D_{56}	D_{44},D_{55}	D_{45},D_{54}	D_{46},D_{53}	D_{47},D_{52}	D_{48},D_{51}
$\sigma(\mathbf{x},t)$	0.0645	0.0499	0.07	0.1294	0.07	0.0499	0.0645	0.0538
$\|\|\Delta\mathbf{f}\|\|_\infty$	1.6114	1.6022	1.3157	0.976	1.3019	1.5798	1.6084	1.3816

A. *Case for* $n_1 = n_2 = 5$

In this case, we select the 25 operating points to be

$$\left\{\mathbf{x}_{ij}=(x_{1,i},x_{2,j},0,0)^T | x_{1,i},x_{2,j}=-\pi/2,-\pi/4,0,\pi/4,\pi/2\right\}. \tag{29}$$

According to the selected operating points and letting $\mathbf{f}(\mathbf{x}) = A(\mathbf{x})\mathbf{x}$, we have

$$\begin{aligned}
(A(\mathbf{x}))_{11} &= \frac{(m_1+m_2)gs_1}{l_1a_2x_1}\\
(A(\mathbf{x}))_{12} &= -\frac{m_2ga_3s_2}{l_1a_2x_2}\\
(A(\mathbf{x}))_{13} &= m_2l_1l_2a_1a_3x_3\\
(A(\mathbf{x}))_{14} &= -m_2l_2^2a_1x_4\\
(A(\mathbf{x}))_{21} &= \frac{(m_1+m_2)ga_3s_1}{l_2a_2x_1}\\
(A(\mathbf{x}))_{22} &= \frac{(m_1+m_2)gs_2}{l_2a_2x_2}\\
(A(\mathbf{x}))_{23} &= (m_1+m_2)l_1^2a_1x_3\\
(A(\mathbf{x}))_{24} &= m_2l_1l_2a_1a_3x_4.
\end{aligned}$$

The overall of associated 25 linear models can then be easily obtained. Two of them are listed as follows:

$$A_{11} = \begin{pmatrix} 12.4777 & -6.2389 & 0 & 0\\ -12.4777 & 12.4777 & 0 & 0\end{pmatrix}$$

$$B_{11} = \begin{pmatrix} 1 & -1\\ -1 & 2\end{pmatrix}$$

$$A_{12} = \begin{pmatrix} 8.3185 & -4.1592 & 0 & 0\\ -5.8821 & 11.7641 & 0 & 0\end{pmatrix}$$

$$B_{12} = \begin{pmatrix} 0.6667 & -0.4714\\ -0.4714 & 1.3333\end{pmatrix}$$

where (A_{ij},B_{ij}) denotes the linear model associated with the operating point $\mathbf{x}_{ij}$. After determining the 25 linear models, the T–S fuzzy system model can be easily determined when the angular positions of the robot are available. Define the region $D_{ij} := \{\mathbf{x}|x_{1,i}\le x_1\le x_{1,i+1}, x_{2,j}\le x_2\le x_{2,j+1}, -1\le x_3,x_4\le 1\}$. The upper bounds of $\sigma(\mathbf{x},t)$ and $\|\Delta\mathbf{f}\|_\infty := \sup_{\mathbf{x}\in D_{ij}}\|\mathbf{f}(\mathbf{x})\|$ over the region D_{ij} can be off-line computed, as given in Table I.

B. *Case for* $n_1 = n_2 = 9$

There are 81 operating points for this case, which are selected to be in the form of the following:

$$\left\{\mathbf{x}_{ij}=(x_{1,i},x_{2,j},0,0)^T | x_{1,i},x_{2,j}=k\pi/8, k=0,\pm1,\ldots,\pm4\right\}. \tag{30}$$

Following the same procedure as that of the previous case, the associated 81 linear models can also be easily obtained. The upper bounds of $\sigma(\mathbf{x},t)$ and $\|\Delta\mathbf{f}\|_\infty$ over the region D_{ij} can be off-line calculated, as given in Table II. It is clear from these two tables that the upper bounds for these uncertainties are decreasing as the partitions of the workspace get finer.

Numerical simulation results are summarized in Table III and Figs. 4–6. Among these, Table III shows the performances under three different reference trajectories, while Figs. 4–6 display the time responses of the tracking errors, the control efforts, and the sliding variables, respectively, for the first reference trajectory described in Table III. In this paper, we use the following three control schemes: One is the classic SMC control design (21) (labeled as Classic SMC), and the other two are the T–S model-based SMC control schemes (14), (15), and (19) with the workspace being partitioned according to Cases A and B (labeled by TS55+SMC and TS99+SMC). The control parameters are set to be $K = I$ and $\eta = 1$, and the sign function is replaced with the saturation function $\text{sat}(s/\nu)$, $\nu = 0.005$ for all of the three control schemes. In addition, we assume that the disturbance that includes viscous and Coulomb frictional forces is adopted from [20] as $\mathbf{d} = (0.1\sin(10t) + f_{v_1}x_3 + f_{C_1}, 0.1\cos(15t) + f_{v_2}x_4 + f_{C_2})^{\mathrm{T}}$, where $f_{v_1} = -0.00148$,

TABLE III
PERFORMANCES OF THE THREE SMC SCHEMES WITH DIFFERENT REFERENCE TRAJECTORIES

	Case 1 $\mathbf{x}_0 = [0.8, -0.4, 1, 1]^T$ $\mathbf{x}_d = [0.1, -0.7, 0, 0]^T$			Case 2 $\mathbf{x}_0 = [-0.2, -1.1, -2, -2]^T$ $\mathbf{x}_d = [0.7, -0.8, 0, 0]^T$			Case 3 $\mathbf{x}_0 = [-0.2, -1.1, 0.01, 0.01]^T$ $\mathbf{x}_d = [0.7, -0.8, 0, 0]^T$		
	$\|\mathbf{u}\|_\infty$	$\int \mathbf{u}^T\mathbf{u}$	$\int \mathbf{e}^T\mathbf{e}$	$\|\mathbf{u}\|_\infty$	$\int \mathbf{u}^T\mathbf{u}$	$\int \mathbf{e}^T\mathbf{e}$	$\|\mathbf{u}\|_\infty$	$\int \mathbf{u}^T\mathbf{u}$	$\int \mathbf{e}^T\mathbf{e}$
Classic SMC	21.57	859.24	1.04	23.75	2089	4.02	15.04	1787.2	0.64
TS55+SMC	47.01	8 02.65	0.40	48.04	2185.5	0.93	37.21	1861.7	0.49
TS99+SMC	30.04	759.71	0.52	33.52	2061.8	1.24	25.29	1829.8	0.51

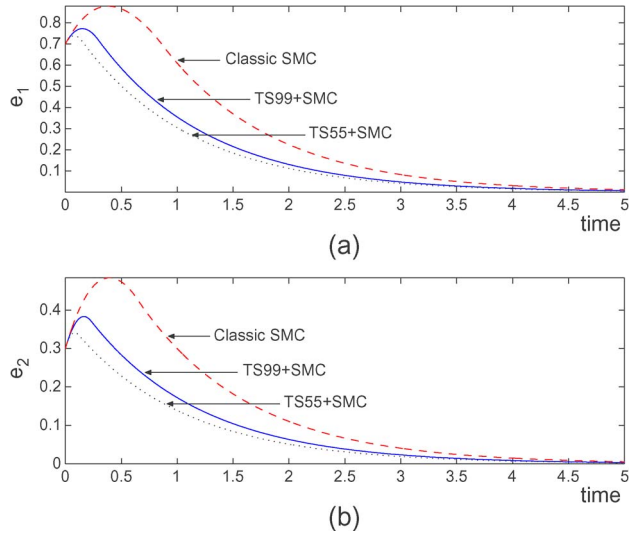

Fig. 4. Time history of the tracking errors.

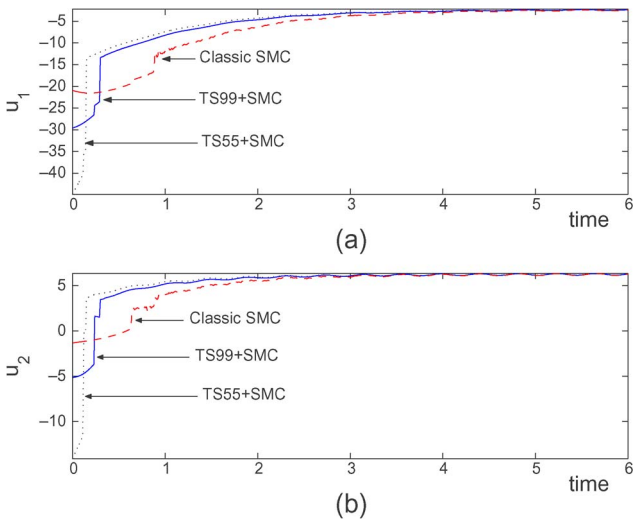

Fig. 5. Time history of the control inputs.

$f_{v_2} = -0.000817$, $f_{C_1} = -0.395$ if $x_3 > 0$, $f_{C_1} = 0.435$ if $x_3 < 0$, $f_{C_2} = -0.126$ if $x_4 > 0$, and $f_{C_2} = 0.071$ if $x_4 < 0$. As expected, it is observed from Fig. 4 that all of the three tracking errors converge to zero. Since the T–S-type SMC schemes need an extra control effort to compensate for the model uncertainties between the T–S and the original nonlinear models, the convergence speed for the T–S-type SMC schemes is found in Fig. 4 to be faster than that of the classic SMC scheme. On the other hand, in (19), the control magnitude of the T–S-type SMC

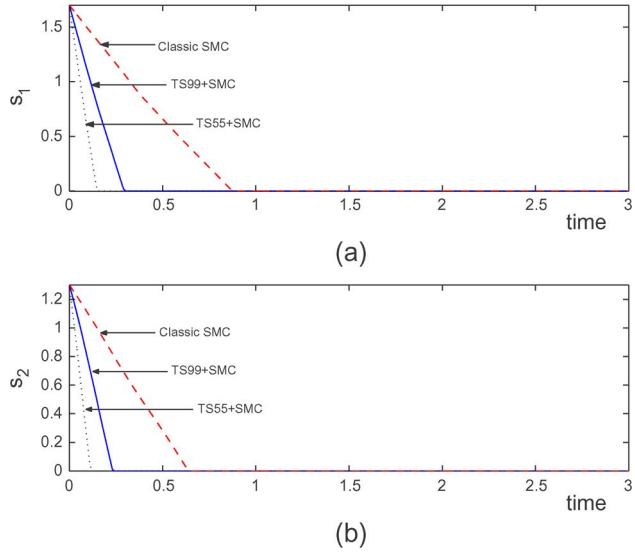

Fig. 6. Time history of the sliding variables.

scheme depends on the size of $\rho(\mathbf{x}, t)$ and $\sigma(\mathbf{x}, t)$, which, in turn, depends on the partition of the workspace. The maximum control magnitude for the three schemes is found in Fig. 5 and Table III to be $(\|\mathbf{u}\|_\infty)_{\text{Classic}} < (\|\mathbf{u}\|_\infty)_{\text{TS99}} < (\|\mathbf{u}\|_\infty)_{\text{TS55}}$, where $\|\mathbf{u}\|_\infty := \sup_t \|\mathbf{u}(t)\|$. Clearly, the finer the partition of the workspace, the smaller the upper bounds $\|\mathbf{f}\|_\infty$, $\sigma(\mathbf{x}, t)$ and the maximum control magnitude of the T–S model-based SMC scheme will be. Thus, the convergence speed of the three schemes has the following relation: $(\text{Speed})_{\text{TS55}} > (\text{Speed})_{\text{TS99}} > (\text{Speed})_{\text{Classic}}$, which can be clearly observed in Fig. 4. Although the T–S approaches need a larger maximum control magnitude than the classic SMC design, they might consume less energy and experience smaller error histories, as shown in Table III. It is also worth noting from Fig. 5 that there are two jumps for all of the three control curves. These jumps correspond to the time instants when the system states reach the sliding surface, which can also be identified in Fig. 6. Finally, when repeatedly computing the controllers 10^6 times, the T–S-type design (including the determination of membership weightings) consumes less CPU time than the classic SMC approach in the relation of $(\text{CPU})_{\text{TS}} \approx 4.766$ s $< (\text{CPU})_{\text{Classic}} \approx 7.625$ s. From these simulations, it is evident that the proposed T–S-type approach not only alleviates the online computational burden but also efficiently supports the tracking control mission as that of the classic SMC design. Moreover, the T–S model-based SMC schemes do not create an extra online computational burden when the number of the fuzzy rules increases.

V. Conclusion

In this paper, we have employed the T–S fuzzy system model approach and the SMC technique to construct a class of robust controllers. The combined scheme is shown to have the following three characteristics. First, the presented scheme can greatly alleviate the online computational burden since it uses the T–S fuzzy system model to approximate the nonlinear model of which most of the system parameters can be obtained offline. Second, the proposed scheme has the advantages of rapid response and robustness as conventional SMC schemes because it adopts the SMC schemes to compensate for the external disturbances and the model uncertainties between the nonlinear and T–S fuzzy system models. Finally, the increase in the number of fuzzy rules by finer partitioning of the workspace can reduce the control magnitude to fulfill the maximum control magnitude constraint for practical applications without creating extra online computational burden. The simulation results for the control of robot manipulators clearly demonstrate the efficiency and the benefits of the presented scheme.

References

[1] G. Bartolini, A. Ferrara, E. Usai, and V. I. Utkin, "On multi-input chattering-free second-order sliding mode control," *IEEE Trans. Ind. Electron.*, vol. 45, no. 9, pp. 1711–1717, Sep. 2000.

[2] A. Bartoszewicz, "Discrete-time quasi-sliding-mode control strategies," *IEEE Trans. Ind. Electron.*, vol. 45, no. 4, pp. 633–637, Aug. 1998.

[3] I. Batyrshin, O. Kaynak, and I. Rudas, "Fuzzy modeling based on generalized conjunction operations," *IEEE Trans. Fuzzy Syst.*, vol. 10, no. 5, pp. 678–683, Oct. 2002.

[4] M. L. Corradini and G. Orlando, "Actuator failure identification and compensation through sliding modes," *IEEE Trans. Control Syst. Technol.*, vol. 15, no. 1, pp. 184–190, Jan. 2007.

[5] C.-C. Cheng and S.-H. Chien, "Adaptive sliding mode controller design based on T–S fuzzy system models," *Automatica*, vol. 42, no. 6, pp. 1005–1010, Jun. 2006.

[6] K.-H. Cheng, C.-F. Hsu, C.-M. Lin, T.-T. Lee, and C. Li, "Fuzzy–neural sliding-mode control for DC–DC converters using asymmetric Gaussian membership functions," *IEEE Trans. Ind. Electron.*, vol. 54, no. 3, pp. 1528–1536, Jun. 2007.

[7] M. O. Efe, O. Kaynak, and B. M. Wilamowski, "Stable training of computationally intelligent systems by using variable structure systems technique," *IEEE Trans. Ind. Electron.*, vol. 47, no. 2, pp. 487–496, Apr. 2000.

[8] F. Esfandiari and H. K. Khalil, "Stability analysis of a continuous implementation of variable structure control," *IEEE Trans. Autom. Control*, vol. 36, no. 5, pp. 616–620, May 1991.

[9] G. Feng, "A survey on analysis and design of model-based fuzzy control systems," *IEEE Trans. Fuzzy Syst.*, vol. 14, no. 5, pp. 676–697, Oct. 2006.

[10] F.-H. Hsiao, J.-D. Hwang, C.-W. Chen, and Z.-R. Tsai, "Robust stabilization of nonlinear multiple time-delay large-scale systems via decentralized fuzzy control," *IEEE Trans. Fuzzy Syst.*, vol. 13, no. 1, pp. 152–163, Feb. 2005.

[11] C.-L. Hwang, "A novel Takagi–Sugeno-based robust adaptive fuzzy sliding-mode controller," *IEEE Trans. Fuzzy Syst.*, vol. 12, no. 5, pp. 676–687, Oct. 2004.

[12] H. K. Khalil, *Nonlinear Systems*, 3rd ed. Englewood Cliffs, NJ: Prentice-Hall, 2002.

[13] S. Khoo, Z. Man, and S. Zhao, "Sliding mode control of fuzzy dynamic systems," in *Proc. ICARCV*, Singapore, Dec. 5–8, 2006, pp. 1–6.

[14] K.-Y. Lian, C.-H. Chiang, and H.-W. Tu, "LMI-based sensorless control of permanent-magnet synchronous motors," *IEEE Trans. Ind. Electron.*, vol. 54, no. 5, pp. 2769–2778, Oct. 2007.

[15] Y.-W. Liang and S.-D. Xu, "Reliable control of nonlinear systems via variable structure scheme," *IEEE Trans. Autom. Control*, vol. 51, no. 10, pp. 1721–1725, Oct. 2006.

[16] Y.-W. Liang, S.-D. Xu, and C.-L. Tsai, "Study of VSC reliable designs with application to spacecraft attitude stabilization," *IEEE Trans. Control Syst. Technol.*, vol. 15, no. 2, pp. 332–338, Mar. 2007.

[17] D.-C. Liaw and J.-T. Huang, "Contact friction compensation for robots using genetic learning algorithm," *J. Intell. Robot. Syst.*, vol. 23, no. 2–4, pp. 331–349, Oct. 1998.

[18] F.-J. Lin, L.-T. Teng, and P. H. Shieh, "Intelligent sliding-mode control using RBFN for magnetic levitation system," *IEEE Trans. Ind. Electron.*, vol. 54, no. 3, pp. 1752–1762, Jun. 2007.

[19] C. Lin, Q.-G. Wang, and T. H. Lee, "Stabilization of uncertain fuzzy time-delay systems via variable structure control approach," *IEEE Trans. Fuzzy Syst.*, vol. 13, no. 6, pp. 787–798, Dec. 2005.

[20] C.-K. Lin, "Nonsingular terminal sliding mode control of robot manipulators using fuzzy wavelet networks," *IEEE Trans. Fuzzy Syst.*, vol. 14, no. 6, pp. 849–859, Dec. 2006.

[21] J.-J. E. Slotine and W. Li, *Applied Nonlinear Control*. Englewood Cliffs, NJ: Prentice-Hall, 1991.

[22] M. W. Spong and M. Vidyasagar, *Robot Dynamics and Control*. New York: Wiley, 1989.

[23] C.-Y. Su and T.-P. Leung, "A sliding mode controller with bounded estimation for robot manipulators," *IEEE Trans. Robot. Autom.*, vol. 9, no. 2, pp. 208–214, Apr. 1993.

[24] C.-H. Sun and W.-J. Wang, "An improved stability criterion for T–S fuzzy discrete systems via vertex expression," *IEEE Trans. Syst., Man, Cybern. B, Cybern.*, vol. 36, no. 3, pp. 672–678, Jun. 2006.

[25] F. Sun, L. Li, H.-X. Li, and H. Liu, "Neuro-fuzzy dynamic-inversion-based adaptive control for robotic manipulators—Discrete time case," *IEEE Trans. Ind. Electron.*, vol. 54, no. 3, pp. 1342–1351, Jun. 2007.

[26] T. Takagi and M. Sugeno, "Fuzzy identification of systems and its applications to modeling and control," *IEEE Trans. Syst., Man, Cybern.*, vol. SMC-15, no. 1, pp. 116–132, Jan./Feb. 1985.

[27] K. Tanaka and H. O. Wang, *Fuzzy Control Systems Design and Analysis: A Linear Matrix Inequality Approach*. New York: Wiley, 2001.

[28] C.-S. Tseng, B.-S. Chen, and H.-J. Uang, "Fuzzy tracking control design for nonlinear dynamic systems via T–S fuzzy model," *IEEE Trans. Fuzzy Syst.*, vol. 9, no. 3, pp. 381–392, Jun. 2001.

[29] R.-J. Wai, "Fuzzy sliding-mode control using adaptive tuning technique," *IEEE Trans. Ind. Electron.*, vol. 54, no. 1, pp. 586–594, Feb. 2007.

[30] X. Yu, Z. Man, and B. Wu, "Design of fuzzy sliding-mode control systems," *Fuzzy Sets Syst.*, vol. 95, no. 3, pp. 295–306, May 1998.

[31] Y. Zhang, S. S. Ge, and T. H. Lee, "A unified quadratic-programming-based dynamical system approach to joint torque optimization of physically constrained redundant manipulators," *IEEE Trans. Syst., Man, Cybern. B, Cybern.*, vol. 34, no. 5, pp. 2126–2132, Oct. 2004.

[32] F. Zheng, Q.-G. Wang, and T. H. Lee, "Output tracking control of MIMO fuzzy nonlinear systems using variable structure control approach," *IEEE Trans. Fuzzy Syst.*, vol. 10, no. 6, pp. 686–697, Dec. 2002.

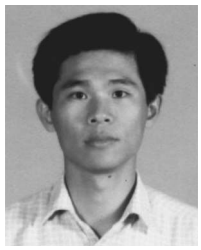

Yew-Wen Liang (M'02) was born in Taiwan in 1960. He received the B.S. degree in mathematics from Tunghai University, Taichung, Taiwan, in 1982, and the M.S. degree in applied mathematics and the Ph.D. degree in electrical and control engineering from National Chiao Tung University, Hsinchu, Taiwan, in 1984 and in 1998, respectively.

Since August 1987, he has been with National Chiao Tung University, where he is currently an Associate Professor in the Department of Electrical and Control Engineering. His research interests include nonlinear control systems, reliable control, and fault detection and diagnosis issues.

Sheng-Dong Xu (S'02) received the B.S. degree in electrical engineering from Yuan Ze Institute of Technology, Chungli, Taiwan, in 1994, and the M.S. degree in biomedical engineering from National Cheng Kung University, Tainan, Taiwan, in 2000. He is currently working toward the Ph.D. degree in the Department of Electrical and Control Engineering, National Chiao Tung University, Hsinchu, Taiwan.

His research interests include control systems, signal processing, and industrial electronics.

Der-Cherng Liaw (S'86–M'90–SM'02) received the B.S. degree in control engineering from National Chiao Tung University (NCTU), Hsinchu, Taiwan, in 1982, the M.S. degree in electrical engineering from National Taiwan University, Taipei, Taiwan, in 1985, and the Ph.D. degree in electrical engineering from the University of Maryland, College Park, in 1990.

During 1990–1991, he was a Postdoctoral Fellow with the Institute of Systems Research, University of Maryland. Since August 1991, he has been with NCTU, where he is currently a Professor in the Department of Electrical and Control Engineering. His research interests include nonlinear control systems, spacecraft control, singular perturbation methods, bifurcation control, jet engine control, flight control, electric power systems and power electronics, radio frequency identification, and implementation issues.

Dr. Liaw served as a Designated Assistant to the Associate Editor for the IEEE TRANSACTIONS ON AUTOMATIC CONTROL during 1990–1992 and was also a Member of the Editorial Board of the 1993 American Control Conference.

Cheng-Chang Chen received the M.S. degree in electrical and control engineering from National Chiao Tung University, Hsinchu, Taiwan, in 2008.

He is currently an Engineer with China Steel Corporation, Taiwan. His research interests include control systems, signal processing, and industrial electronics.